Current-dependent Ocular Tilt Reaction in STN-DBS: evidence for a putative incerto-interstitial pathway?

Maximilian Friedrich (Friedrich_M6@ukw.de)
University Hospital Wuerzburg, Dept. of Neurology, Josef-Schneider- Strasse 11, 97080 Wuerzburg, Germany https://orcid.org/0000-0002-3695-1268

Hazem Eldebakey
University Hospital Wuerzburg, Dept. of Neurology, Josef-Schneider- Strasse 11, 97080 Wuerzburg, Germany

Andreas Zwergal
2. University Hospital Munich, Department of Neurology, Ludwig Maximilian University (LMU), Munich, Germany; 3. German Center for Vertigo and Balance Disorders, DSGZ, LMU Munich, Munich, Germany

Jonas Roothans
University Hospital Wuerzburg, Dept. of Neurology, Josef-Schneider- Strasse 11, 97080 Wuerzburg, Germany

Philipp Capetian
University Hospital Wuerzburg, Dept. of Neurology, Josef-Schneider- Strasse 11, 97080 Wuerzburg, Germany

Jens Volkmann
University Hospital Wuerzburg, Dept. of Neurology, Josef-Schneider- Strasse 11, 97080 Wuerzburg, Germany

Martin Reich
University Hospital Wuerzburg, Dept. of Neurology, Josef-Schneider- Strasse 11, 97080 Wuerzburg, Germany

---

Case Report

Keywords: Vestibular, Deep Brain Stimulation, Movement Disorders

Posted Date: August 4th, 2021

DOI: https://doi.org/10.21203/rs.3.rs-766052/v1

Version of Record: A version of this preprint was published at European Journal of Neurology on January 23rd, 2022. See the published version at https://doi.org/10.1111/ene.15257.

Abstract

Objective: To report a patient with Parkinson's disease presenting with a combined vestibular, oculomotor and postural syndrome dependent of deep brain stimulation (DBS) of the subthalamic nucleus.

Methods: In a systematic monopolar review, eye, head and trunk position in roll and pitch plane were documented as a function of stimulation amplitude and field direction. Repeat ocular coherence tomography was used to estimate ocular torsion. The interstitial nucleus of Cajal (INC), zona incerta (ZI) and ascending vestibular fiber tracts were segmented on MRI using both individual and normative structural and connectomic data. Thresholded symptom-associated volumes of tissue activated (VTA) were calculated based on documented stimulation parameters.

Results: Ipsilateral ocular tilt reaction and body lateropulsion as well as contralateral torsional nystagmus were elicited by the right electrode in a current-dependent manner and subsided after DBS deactivation. With increasing currents, binocular tonic upgaze and subsequently body retropulsion could be elicited, consistent with an irritative effect on the Interstitial Nucleus of Cajal (INC). Symptom-associated VTA was found to overlap with the dorsal zona incerta (dZI) and the lateral ipsilateral vestibulothalamic tract (IVTT), while lying in close proximity to the medial IVTT and rather distant to the INC proper. As described in non-human primates, a ZI-to-INC, "*incerto-interstitial*" tract (IIT) with contact to the medial-uppermost portion of the VTA could be traced. By ways of directional current steering laterally to both tracts, therapeutic response could be preserved while vestibular side effects were minimized.

Conclusion: Unilateral stimulation of mesencephalic vestibular-related circuitry induces an ipsilateral vestibular, oculomotor and postural roll-plane syndrome, which converts into a combined pitch-plane syndrome, when functional activation expands to the bilateral INC. The phenomenology of the roll-plane syndrome in this patient points to an activation of INC neurons by DBS, hypothetically via a potentially aberrant incerto-interstitial pathway. Directional current steering proved useful in managing this rare side effect.

Introduction

Deep brain stimulation (DBS) is an established treatment in movement disorders. Connectomic approaches using "volume of tissue activated" (VTA) models shape understanding of DBS action on functional networks and may help optimizing treatment efficacy[1]. In single cases, subtle vestibulo-perceptive signs like deviations of subjective visual vertical (SVV) have been reported after DBS[2]. Vestibular-oculomotor (VOM) and postural side effects, however, are highly unusual, likely due to stimulation targets lying remote of VOM reflex arcs.

Case Description

History

Since DBS implantation (Boston Scientific® Gevia/ Cartesia) one year prior, a 58-year-old patient reported to perceive “poles tilted like the Tower of Pisa”. He noticed a rightward head tilt and falling to the right but denied vertigo, diplopia, or other focal neurological signs.

Clinical and quantitative neuro-otological and -ophthalmological examination

In the medication/stimulation *ON* state, a left-dominant hypokinetic-rigid syndrome (Unified Parkinson’s Disease Rating Scale III (UPDRS-III) 14 points, DBS improvement in meds-off 62%), rightward head tilt and lateropulsion besides difficulties in tandem walking were noted. Neuro-ophthalmological assessment confirmed a rightward ocular tilt reaction (OTR) with conjugate 10° counterclockwise ocular torsion and binocular rightward 10° SVV deviation. Ocular coherence tomography disclosed residual counterclockwise ocular torsion of -9.5°/-2.1° (right/left eye) shortly after DBS deactivation decreasing to -4.7°/0.6° after overnight withdrawal (Fig. 1A). Apparative otoneurological assessment was unremarkable.

DBS programming

Monopolar review (130Hz, 60µs) revealed that OTR was influenced exclusively and reproducibly by contact 14 (facing supero-postero-medially) of the right lead. OTR magnitude could be modulated linearly starting from 5° * rightward SVV deviation at 1.8mA to approximately 10° at 2.2mA and 25° at 4.5mA (Fig. 1B) accompanied by increasing rightward lateropulsion, skew deviation, and a torsional nystagmus beating to the left (*Supplementary Video*). Upon further increase, binocular tonic upgaze and diagonal lateropulsion evolved into retropulsion, requiring the exploration to be stopped immediately. The patient felt “being drawn rightwards”. Anterolateral current steering on the same level reduced vestibular effects (7° SVV) while preserving antiparkinsonian effects (UPDRS-III 12 points).

Imaging and VTA modelling

Cranial CT disclosed no intracranial pathologies but an obtuse and caudal trajectory of the right electrode. Lead localization and VTA modelling (Fig. 2) showed VOM-syndrome related VTA extending supero-postero-medially (Fig. 1B, C, D).

Discussion

Albeit the VTA overlapping with the iVTT (Fig. 1C, D), the evolving VOM-syndrome and degree of SVV deviation[2] argue against the iVTT as its sole correlate. The oculomotor and postural findings can more likely be related to the INC, which is involved in eye and head coordination in the roll and pitch plane[4].

Unilateral damage of ascending vestibular projections to the INC at midbrain level induce a contralesional OTR, while damage of the INC per se additionally results in ipsilesional torsional nystagmus[5]. In contrast, stimulation of the riMLF seems unlikely, since it would generate an ipsilateral torsional nystagmus[5]. Given the binocularity of oculomotor signs in absence of double vision, 3rd and 4th cranial nerve involvement can be excluded. Hence, we reason that the current-dependent OTR ipsilateral to the stimulation site may be generated by modulation of projections targeting the INC, while contralateral torsional nystagmus at higher currents speaks for additional activation of integrator neurons directly in the INC[5]. Given the neuroanatomical modelling, we hypothesize INC modulation in this patient through a potentially aberrant "*incerto-interstitial*" projection, first described in primates[6] (Fig. 1C). Moreover, simultaneous modulation of medial and lateral iVTT axons may then contribute to the enormous SVV deviation, in line with theoretical considerations of tissue-dependent differential effects of DBS[7].

Increasing upgaze and body retropulsion implicates bilateral INC involvement. Given the topographical relations, direct current spread over the midline can be excluded as a mechanism. With dense posterior commissure projections interconnecting the bilateral INC, synaptic mechanisms for signal transmission to the contralateral INC could be assumed. The transition of ocular and postural symptoms from roll to pitch plane with increase of stimulation currents is consistent with the "double roll = pitch" framework[4].

These case-based findings should of course be interpreted with caution and confirmed in prospective studies, potentially correlating fine-grain oculomotor assays to VTA locations. Nonetheless, this case has three relevant aspects: 1) It gives mechanistic insight into the functional anatomy of plane-specific control of eye, head and body position in the midbrain, 2) allows inferences about modes of action of DBS in sensorimotor circuits and 3) underscores the utility of directional DBS for optimizing treatment efficacy.

References

1. Reich, M. M. *et al.* Probabilistic mapping of the antidystonic effect of pallidal neurostimulation: A multicentre imaging study. *Brain* **142**, (2019).

2. Shaikh, A. G., Antoniades, C., Fitzgerald, J. & Ghasia, F. F. Effects of deep brain stimulation on eye movements and vestibular function. *Frontiers in Neurology* vol. 9 444 (2018).

3. Jang, S. H. & Kwon, H. G. The ipsilateral vestibulothalamic tract in the human brain. *Translational Neuroscience* vol. 9 22–25 (2018).

4. Brandt, T. & Dieterich, M. Central vestibular syndromes in roll, pitch, and yaw planes: Topographic diagnosis of brainstem disorders. *Neuro-Ophthalmology* **15**, (1995).

5. Büttner, U., Büttner-Ennever, J. A., Rambold, H. & Helmchen, C. The contribution of midbrain circuits in the control of gaze. in *Annals of the New York Academy of Sciences* vol. 956 99–110 (New York Academy of Sciences, 2002).

6. Kokkoroyannis, T., Scudder, C. A., Balaban, C. D., Highstein, S. M. & Moschovakis, A. K. Anatomy and physiology of the primate interstitial nucleus of cajal: I. Efferent projections. *Journal of Neurophysiology* **75**, 725–739 (1996).

7. Ashkan, K., Rogers, P., Bergman, H. & Ughratdar, I. Insights into the mechanisms of deep brain stimulation. *Nature Reviews Neurology* vol. 13 548–554 (2017).

Declarations

Ethics approval and consent to participate and disclose:

Patient gave informed written consent to consent, disclose and for publication of this retrospective study.

Data availability:

Non-identifiable data is available upon reasonable request to the corresponding author.

Competing interests:

Authors declare no conflicts of interest pertaining to the manuscript.

Funding:

Dr. Maximilian U. Friedrich receives funding from the Interdisciplinary Center for Clinical Research (IZKF) Z2-CSP13 at the University Hospital Wuerzburg.

Authors' contributions:

MF obtained and analyzed patient data, conceptualized, drafted and revised the manuscript. HD analyzed patient data and drafted the manuscript. JR analyzed patient data. AZ analyzed patient data and revised the manuscript. PC obtained patient data. MR and JV obtained patient data and revised the manuscript.

Acknowledgements:

The authors want to thank Dr. Miriam Buerklein (University Hospital Wuerzburg, Dept. of Otorhinolaryngology) and Christoph Kalantari, FEBO (University Hospital Wuerzburg, Dept. of Ophthalmology) for their assistance in neuro-otological and neuro-ophthalmologic assessments as well as Prof. Dr. Anja Horn-Bochtler (University Munich, Institute of Anatomy and Cell Biology) for the fruitful discussion.

Supplementary Methods

The subject's preoperative T1 and T2 MRI images were fused with the postoperative CT in Brainlab Elements software (Brainlab AG, Munich, Germany). Leads were manually localized based on their

artifacts and their rotational orientation determined by Brainlab algorithm. Volume of tissue activated (VTA) were calculated based on the stimulation parameters and configuration. Extraction and normalization of the VTAs from the patients native space into the common MNI; ICBM 2009b NLIN asymmetric brain space (Fonov et al., 2009, 2011) as done by an in-house built toolbox in Matlab environment (in part publicly available at: https://github.com/JonasRoothans/ArenaToolbox), which makes use of the unified tissue segmentation (Ashburner & Friston, 2005) in SPM12 (statistical Parametric Mapping, http://www.fil.ion.ucl.ac.uk/spm/software/spm12/).

Segmentation of the ipsilateral vestibulothalamic tract (iVTT) and tract from Interstitial Nucleus of Cajal (INC) to Zona incerta.

To reconstruct the ipsilateral vestibulothalamic tract, we segmented the vestibular nucleus in Mango (Multi-Image analysis GUI, http://ric.uthscsa.edu/mango/) on the fractional anisotropy template of the MNI; ICBM 2009b NLIN asymmetric brain space in a similar manner as previously described (Jang & Kwon, 2018), while depending on the posterior, medial and lateral anatomical boundaries for segmenting the vestibular nucleus in the shape of a square prism with the long dimension along the vertical axis and otherwise equal sides of 5 mm . We then performed fiber-tracking in DSI studio using the HCP1021 template (http://brain.labsolver.org/diffusion-mri-templates/hcp-842-hcp-1021). The template represents the averaged voxel-based spin distribution functions of subjects from the human connectome project allowing for fiber reconstruction based on the regions of interest and tracking parameters (Van Essen et al., 2012; Yeh et al., 2010; Yeh & Tseng, 2011)

The right vestibular nucleus was set as a seed and the right thalamus from the automated anatomical labelling atlas 3 (Rolls et al., 2020) as a region of interest. We used the following parameters: 100,000 seeds, QA threshold: 0.25, angular threshold of 52 degrees and using Euler's deterministic fiber-tracking algorithm with a step size of 0.5 mm. For visualization purposes the INC was segmented on a T1 structural template (MNI; ICBM 2009b NLIN asymmetric) in Mango with aid of relations to neighboring neuroanatomical structures as depicted in Allen human brain atlas (http://www.atlas.brain-map.org) with the help of HCP842 tractography atlas (Yeh et al., 2018) where appropriate. The zona incerta was acquired from supplementary files of published literature (Lau et al., 2020). The INC was used as seed and zona incerta as a region of interest for fiber-tracking in DSI studio using the HCP1021 template with the following parameters: 100,000 seeds, QA threshold: 0.20, angular threshold of 52 degrees and using Euler's deterministic fiber-tracking algorithm with a step size of 0.5 mm. The tracts and anatomical structures of interest were then visualized in DSI studio superimposed on a high resolution joint template from T1 & T2 7T MRIs of an ex-vivo brain normalized to MNI space (Edlow et al., 2019).

Supplementary method references

Ashburner, J., & Friston, K. J. (2005). Unified segmentation. *NeuroImage*, *26*(3), 839–851. https://doi.org/10.1016/j.neuroimage.2005.02.018

Edlow, B. L., Mareyam, A., Horn, A., Polimeni, J. R., Witzel, T., Tisdall, M. D., Augustinack, J. C., Stockmann, J. P., Diamond, B. R., Stevens, A., Tirrell, L. S., Folkerth, R. D., Wald, L. L., Fischl, B., & van der Kouwe, A. (2019). 7 Tesla MRI of the ex vivo human brain at 100 micron resolution. *Scientific Data*, *6*(1), 244. https://doi.org/10.1038/s41597-019-0254-8

Fonov, V., Evans, A. C., Botteron, K., Almli, C. R., McKinstry, R. C., Collins, D. L., & Brain Development Cooperative Group. (2011). Unbiased average age-appropriate atlases for pediatric studies. *NeuroImage*, *54*(1), 313–327. https://doi.org/10.1016/j.neuroimage.2010.07.033

Fonov, V., Evans, A., McKinstry, R., Almli, C., & Collins, D. (2009). Unbiased nonlinear average age-appropriate brain templates from birth to adulthood. *NeuroImage*, *47*, S102. https://doi.org/10.1016/S1053-8119(09)70884-5

Jang, S. H., & Kwon, H. G. (2018). The Ipsilateral Vestibulothalamic Tract in the Human Brain. *Translational Neuroscience*, *9*, 22–25. https://doi.org/10.1515/tnsci-2018-0005

Lau, J. C., Xiao, Y., Haast, R. A. M., Gilmore, G., Uludağ, K., MacDougall, K. W., Menon, R. S., Parrent, A. G., Peters, T. M., & Khan, A. R. (2020). Direct visualization and characterization of the human zona incerta and surrounding structures. *Human Brain Mapping*, *41*(16), 4500–4517. https://doi.org/10.1002/hbm.25137

Rolls, E. T., Huang, C.-C., Lin, C.-P., Feng, J., & Joliot, M. (2020). Automated anatomical labelling atlas 3. *NeuroImage*, *206*, 116189. https://doi.org/10.1016/j.neuroimage.2019.116189

Van Essen, D. C., Ugurbil, K., Auerbach, E., Barch, D., Behrens, T. E. J., Bucholz, R., Chang, A., Chen, L., Corbetta, M., Curtiss, S. W., Della Penna, S., Feinberg, D., Glasser, M. F., Harel, N., Heath, A. C., Larson-Prior, L., Marcus, D., Michalareas, G., Moeller, S., … WU-Minn HCP Consortium. (2012). The Human Connectome Project: A data acquisition perspective. *NeuroImage*, *62*(4), 2222–2231. https://doi.org/10.1016/j.neuroimage.2012.02.018

Yeh, F.-C., Panesar, S., Fernandes, D., Meola, A., Yoshino, M., Fernandez-Miranda, J. C., Vettel, J. M., & Verstynen, T. (2018). Population-averaged atlas of the macroscale human structural connectome and its network topology. *NeuroImage*, *178*, 57–68. https://doi.org/10.1016/j.neuroimage.2018.05.027

Yeh, F.-C., & Tseng, W.-Y. I. (2011). NTU-90: A high angular resolution brain atlas constructed by q-space diffeomorphic reconstruction. *NeuroImage*, *58*(1), 91–99. https://doi.org/10.1016/j.neuroimage.2011.06.021

Yeh, F.-C., Wedeen, V. J., & Tseng, W.-Y. I. (2010). Generalized q-sampling imaging. *IEEE Transactions on Medical Imaging*, *29*(9), 1626–1635. https://doi.org/10.1109/TMI.2010.2045126

Figures

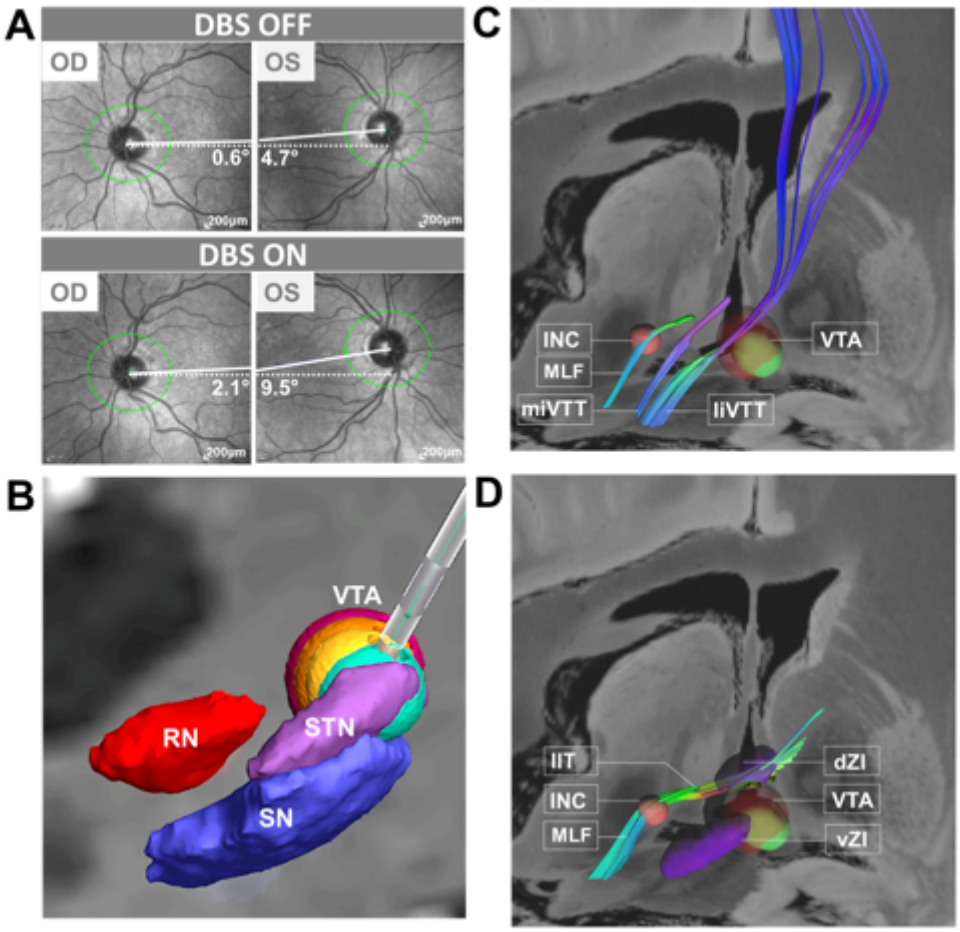

Figure 1

Synopsis of findings. A. OCT shows a significant increase of vertical deviation with the right eye down and a conjugate counterclockwise ocular torsion in DBS on more than off condition. Solid lines delineate the maculo-papillary meridian, dashed lines the approximated true horizontal. B. Electrode localization relative to neuroanatomic landmark structures SN (blue), RN (red) and STN (pink). VOM-related VTA models for amplitudes generating 5° OTR (green), 10° OTR (yellow), additional tonic upgaze (orange) and 20-25° OTR & body retropulsion (dark red) are superimposed on an individual coronal T1w MRI. VOM-related VTAs extend in supero-medial direction. C. Visualization of the VTAs (green: minimal vestibular symptoms; red: maximal vestibular symptoms) relative to the INC as well as the ipsilaterally ascending medial and lateral vestibular white matter tracts conveying vestibulo-perceptive signals to the cortex via the thalamic paramedian and posterolateral nuclei respectively. Note, VTA lies remote of INC and MLF. D. Tracing of an incerto-interstitial fiber tract connecting dorsal zona incerta and ipsilateral INC which is reached by uppermost and medial border of symptom-associated VTA. Abbreviations: CNIII: 3rd cranial nerve, IIT: incerto-interstitial tract, INC: Interstitial Nucleus of Cajal, miVTT/liVTT: medial/ lateral ipsilateral vestibulo-thalamic tract, MLF: medial longitudinal fascicle, OCT: optical coherence tomography, OD: right eye, OS: left eye, OTR: ocular tilt reaction, RN: red nucleus, OTR: ocular tilt reaction, SN: substantia nigra, STN: subthalamic nucleus, VTA: volume of tissue activated, dZI/vZI: dorsal/ ventral zona incerta. See supplemental methods for details.

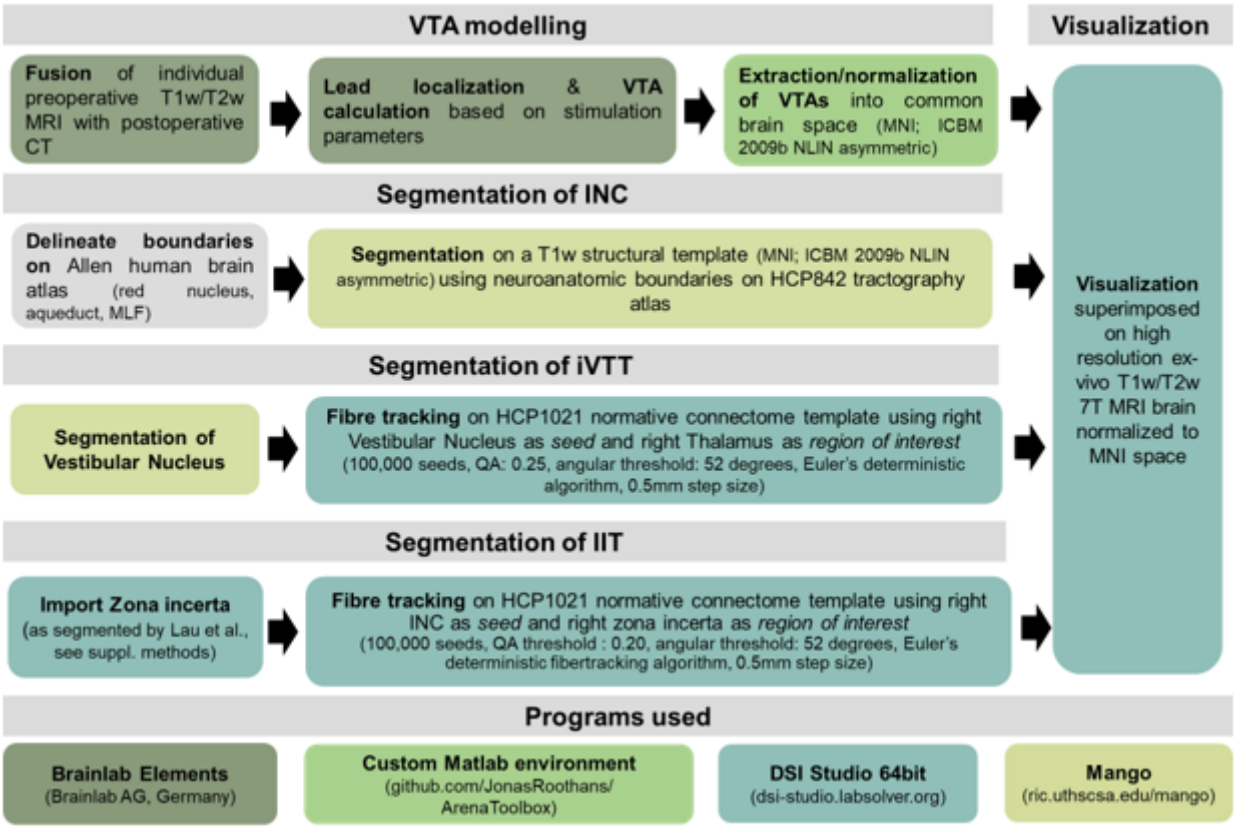

Figure 2

Imaging Workflow for modelling of volume-of-tissue-activated, segmentation of ipsilateral vestibulothalamic (iVTT), incerto-interstitial (IIT) tracts and Interstitial Nucleus of Cajal (INC). Worksteps are color-coded depending on program used.

Supplementary Files

This is a list of supplementary files associated with this preprint. Click to download.

- OTRinSTNDBSVideo.mp4